Journal of Carcinogenesis
Covering Genesis to Therapeutics

Journal of Carcinogenesis, ISSN: 1477-3163
2025; Vol 24: Issue 4s, https://carcinogenesis.com/

Exploring High-Efficiency Organic LEDs for Cancer Biomarker Detection: A Comparative and Functional Analysis

Rajesh Kumar Tiwari[1], Sanjay Kumar Sharma[2], Rajesh Mishra[3], Nakshathra Prabhu[4], Mangey Ram Nagar[5*]

[1, 2, 3]School of Information and Communication Technology, Gautam Buddha University, Greater Noida, India

[4]School of Bioengineering and Biosciences, Lovely Professional University, Phagwara, India

[*5]School of Electronics, Noida Institute of Engineering and Technology, Greater Noida, India

***Corresponding Author:**

Mangey Ram Nagar

Email ID: mangey.nagar@niet.co.in

ABSTRACT

This study presents a performance analysis and comparative evaluation of third-generation thermally activated delayed fluorescence (TADF) organic light-emitting diodes (LEDs) against previous generations of organic-LED technologies. The evolution of organic-LEDs has significantly transformed display, lighting, and biomedical applications, with TADF materials, particularly carbazole derivatives, emerging as promising candidates for achieving high efficiency through the utilization of both singlet and triplet excitons. The research highlights the potential of TADF organic-LEDs in enhancing cancer detection and treatment via photodynamic therapy, showcasing their unique optical properties that improve sensitivity in identifying cancer biomarkers. Despite advancements, challenges such as efficiency roll-off at elevated drive currents persist, necessitating ongoing investigations into material stability, triplet population management, and device architecture optimization. The findings underscore the importance of interdisciplinary collaboration in advancing TADF organic-LED technology, paving the way for innovative applications in personalized medicine and improved therapeutic outcomes. Overall, this study contributes to the foundational understanding required for the continued development and commercialization of TADF organic-LEDs in high-performance applications.

Keywords: *TADF organic-LED; fluorescent materials; phosphorescent materials*

How to Cite: Rajesh Kumar Tiwari, Sanjay Kumar Sharma, Rajesh Mishra, Nakshathra Prabhu, Mangey Ram Nagar, (2025) Exploring High-Efficiency Organic LEDs for Cancer Biomarker Detection: A Comparative and Functional Analysis, *Journal of Carcinogenesis*, *Vol.24, No.4s*, 349-358

1. INTRODUCTION

Through combining organic semiconductors and charge transport layers that enable light emission between transparent electrodes, organic light-emitting diodes (LEDs), have revolutionized the landscape of display, lighting, and biomedical technologies [1-3]. In this framework, charge injection and recombination processes produce singlet and triplet excitons [4]. Conventional fluorescent OLEDs only use singlet excitons to emit light, which led to the creation of phosphorescent materials that can efficiently use triplet emissions to increase device efficiency[5]. The search for a commercially viable blue phosphorescent emitter is still a difficult task, despite the fact that this method has produced notable improvements in red and green light emissions [6].

As a result, thermally activated delayed fluorescence (TADF) has become a viable substitute that makes it possible to use triplet excitons to further increase efficiency. Because of their superior charge transport characteristics and high photoluminescence quantum yields, carbazole derivatives are particularly promising among TADF emitter materials and could be used to create extremely effective organic LEDs [7]. Because of their special optical properties, TADF OLEDs have a lot of potential for both cancer detection and treatment. By precisely identifying cancerous cells and associated biomarkers, these OLEDs can be incorporated into advanced imaging systems or biosensors, increasing the sensitivity for

early detection that is essential for successful treatment outcomes [8]. TADF OLEDs' distinctive delayed fluorescence enhances signal-to-noise ratios, making it easier to detect low biomarker concentrations precisely.

Engineered TADF materials may provide novel phototherapy options in therapeutic settings while reducing collateral damage to healthy tissues; however, issues with material stability and operational efficiency will need to be addressed through continued research [9]. However, the phenomenon of efficiency roll-off at high drive currents remains a significant limitation despite significant advancements in TADF OLED technology.

Both phosphorescent and TADF OLEDs exhibit efficiencies that are more than four times higher than those of their fluorescent counterparts; however, as current density rises, their performance significantly deteriorates, with TADF devices being especially vulnerable to this efficiency loss [10]. In order to overcome the problem of efficiency roll-off, methods for shortening triplet lifetimes or—more importantly—controlling the triplet population while the device is operating are required, opening the door for more reliable and economically feasible OLED technologies [11], [12].To overcome these challenges, it is required to have a deep understanding of the electro-optical characteristics of organic LEDs and precise optimization of device structure.

OLED in Photodynamic Therapy

Organic light-emitting diodes (OLEDs) have been investigated for ovarian cancer detection. A novel OLED structure has been developed to enhance luminescence and efficiency. This sensor detects ovarian cancer by analyzing urine fluorescence, revealing distinct wavelengths and currents in healthy versus cancerous individuals. The authors propose its potential as a portable and cost-effective diagnostic tool [13]. An earlier study emphasized the significance of early cancer detection and introduced a non-invasive OLED sensor for ovarian cancer. The potential for a home-use portable device for early diagnosis was highlighted [14]. Both studies aim to improve survival rates by offering accessible diagnostic solutions. Photodynamic therapy (PDT) is a non-invasive treatment for superficial tumors with low toxicity. PDT employs various photosensitizers (PS) for diverse tumors in anti-tumor applications. PSs are crucial in PDT, activating agents to generate reactive oxygen species (ROS) for inducing apoptosis in tumor cells. First-generation PSs like Photofrin are approved, while research is ongoing for advanced second and third-generation agents. Activatable PSs are being developed to control singlet oxygen production, enhancing PDT selectivity and efficacy.

Table 1. Examples of materials used in different generations of photosensitizers

Generations of PS	Examples
First Generation	Porphyrin, Hematoporphyrin
Second Generation	Benzoporphyrin, 5-ALA, Protoporphyrin IX
Third-generation Generation	Antibody conjugates, TADF

Innovations seek to improve tumor selectivity, ROS generation, and near-infrared absorption for better tissue penetration. Nanoparticle formulations are emerging as a solution to enhance the pharmacokinetics and phototoxicity of traditional PSs. Clinically approved PSs include Photofrin, Foscan, and Visudyne, with ongoing exploration of third-generation variants for improved targeting efficiency. Despite significant progress, challenges remain in treating deep tissue cancers, necessitating further research into PS optimization for oncological applications [15]. The Table.1 below shows the materials used in various generations of photosensitizers (PS).

Generational Advances in OLED Emitters

Organic Light-Emitting Diodes (OLEDs) have evolved through three generations of emitter materials since their introduction in 1987 [16]. The first generation utilized fluorescent materials, followed by phosphorescent materials in the thermally induced delayed fluorescence, and the second generation (TADF) in the third generation [17], [18]. A fourth generation, known as hyperfluorescence, has also emerged. Each generation has improved upon the previous, with advancements in efficiency, stability, color range, and performance. The emitter materials have evolved from traditional fluorescent compounds to metal phosphorescent complexes, including both precious and non-precious metals[8]. Polymer-based OLEDs have attracted attention for their higher stability due to higher glass transition temperatures [17]. The first-generation fluorescent OLEDs (FOLEDs) were based on pure organic materials, while the second and third-generations incorporated organometallic compounds to enhance efficiency. Because of their high efficiency, which comes from spin-orbit coupling, second-generation phosphorescent OLEDs (POLEDs) are frequently used in displays [19]. Even greater efficiency is possible with third-generation TADF-based OLEDs, which could theoretically achieve 100% external quantum efficiency [18], [19]. Novel emitter materials are still being investigated in order to improve OLED performance.

Organic light-emitting diodes (OLEDs) and light-emitting electrochemical cells (LECs) have significantly improved as a result of recent developments in thermally activated delayed fluorescence (TADF) emitters. With adjustable colors and

longer device lifespans, all-fluorescent white OLEDs were able to achieve external quantum efficiencies (EQEs) of over 30% [20]. In hyperfluorescent devices, multiple resonance TADF emitters showed high-performance narrowband electroluminescence with EQEs as high as 42.3% [21]. With EQEs of 7.6% and luminance of 3696 cd m-2, TADF-LECs achieved record efficiencies and luminance through dopant engineering [22]. Efficiency was positively impacted by the chromophores' flexibility in red TADF materials; devices based on PT-TPA achieved maximum EQEs of 29.7% at 632 nm [23]. These studies show the versatility of TADF emitters and offer information on molecular design techniques for high-performance light-emitting devices. The efficiency and emission wavelength of near-infrared (NIR) thermally activated delayed fluorescence (TADF) organic light-emitting diodes (OLEDs) have significantly improved. [24] used a Y-shaped NIR TADF molecule to report a record-high external quantum efficiency (EQE) of 13.2% at 761 nm. Similarly, using their NIR-TADF emitter, TPA-PZTCN, [25] obtained an EQE of 13.4% at 734 nm. showed an asymmetric TADF emitter with exceptional EQEs of 5.4% for NIR emission at 718 nm and 21.9% and 19.2% for red emission. These findings mark a substantial advancement over previous research by [26-27], who discovered the first NIR TADF molecule with an EQE of 10% at 668 nm. Potential uses in biomedical sensing, imaging, and telecommunications are made possible by these developments. The Table below reviews the literature of the papers based on the different generations of OLEDs.

Fabrication of Blue OLEDs

Indium tin oxide (ITO) is first deposited onto a substrate, like glass, using a sputtering technique. This is followed by a number of cleaning procedures in the fabrication process for fluorescent OLED devices. Scrubbing and sonication are used to clean the surface, which is then rinsed in deionized (DI) water and dried in an oven.

Table 2. Comparison of Characteristics of First, Second, and Third Generation OLEDs

S.No	Characteristics	First Gen OLED	Second Gen OLED	Third Gen OLED	Ref
1	Materials used	Alq3, DCM1, DCM2	fac-Ir(ppy)$_3$, Pt- based complexes	4CzTPN-Ph, DTC- DPS	[16]
	Efficiency	Maximum EQE of 5%	IQE up to 100%	Theoretical IQE of 100%	
	Wavelength	Green: 550 nm, Orange-red: 570–650 nm, Blue: 452 nm	Green: 510 nm, 528 nm, Red: 616 nm, 620 nm	Orange-red: 580 nm, 600+ nm; Deep blue: 423 nm, 428 nm; Sky blue: 467– 497 nm	
2	Materials used	DAD conjugated oligomer, im- proved red fluores- cent emitters	Ir(ppy)$_3$ (green), Ir(dmp)$_3$ (blue), Firpic (deep blue)	4CzIPN (green), 2CzPN, DMAC- DPS (blue), NAI-DPAC, NAI-DMAC (orange-red)	[17]
	Efficiency	Fluorescent OLEDs using conductive polymers can achieve satisfactory device perfor- mance.	Phosphorescent OLEDs can achieve 100% IQE by uti-lizing singlet and triplet excitons with Ir-based com-plexes.	TADF OLEDs can theoretically achieve 100% IQE; green and blue emitters show high EQEs (e.g., 19.4% for 4CzIPN); red emitters are less studied.	
	Wavelength	Not provided	Green: 510 nm (Ir(ppy)$_3$), Blue: 475 nm (Firpic)	Blue: Not specified (2CzPN)	
3	Materials used	Tris(8-hydroxyquinoline) aluminium (Alq3)	Iridium-based organometallic compounds such as IrQ(ppy)$_2$	TADF compounds synthesized via Suzuki and nucle- ophilic substitution reactions	[19]
	Efficiency	Based on pure organic materials, with lower effi- ciency	High efficiency due to spin-orbit coupling in metal- ligand complexes	Aims for 100% ex-ternal quantum effi- ciency using TADF	
	Wavelength	Not mentioned	Green: 535 nm, Red: 607–670 nm (by tuning ligands)	Not mentioned	
4	Materials used			Two Y-shaped NIR TADF molecules: Py-TPA and Py- CN-TPA	[24]
	Efficiency			13.2%	
	Wavelength			726 nm, 747 nm, 761 nm; EQE of 22.2% at 726 nm (in thin film)	
	Electrical characteris- tics			The emitters exhibit an EQE of 22.2% at 726nm, within this film.	

The ITO substrate may occasionally be further cleaned using methods like plasma treatment or ethanol and acetone treatment followed by 15 minutes of ultraviolet (UV) light, depending on the specific requirements and material availability. After that, the thoroughly cleaned ITO/glass substrate is covered with various organic layers using spin coating or vacuum evaporation techniques. The vacuum evaporation process uses high vacuum conditions (10-6 to 10-7 Torr) and

temperatures between 60 and 80◦C. The material to be deposited is dissolved in a suitable solvent before employing the spin coating method. The solution is then spin-coated onto the substrate and dried to facilitate solvent evaporation. A range of methods, such as oscillating quartz thickness monitors, are used to meticulously track the thickness of each layer. The organic layer utilized in this reference device is poly(3,4-ethylenedioxythiophene): poly(styrene sulfonate) (PEDOT: PSS). The hole transport layer is NPB (N,N'-Di(1-naphthyl)-N,N'-diphenyl-(1,10-biphenyl)-4,4' diamine), while the electron injection and transport layer is BPhen. DPVBi is included as the emission layer along with BCzVBi. Finally, the cathode—a LiF and Al bilayer—is thermally deposited. Deposition typically occurs at low temperatures because high-temperature operations could compromise the integrity of the organic materials. Deposition is therefore done at high vacuum and low temperatures (60–80°C). Device analyses follow, in which the outcomes of the experimental device and the manufactured device are compared.

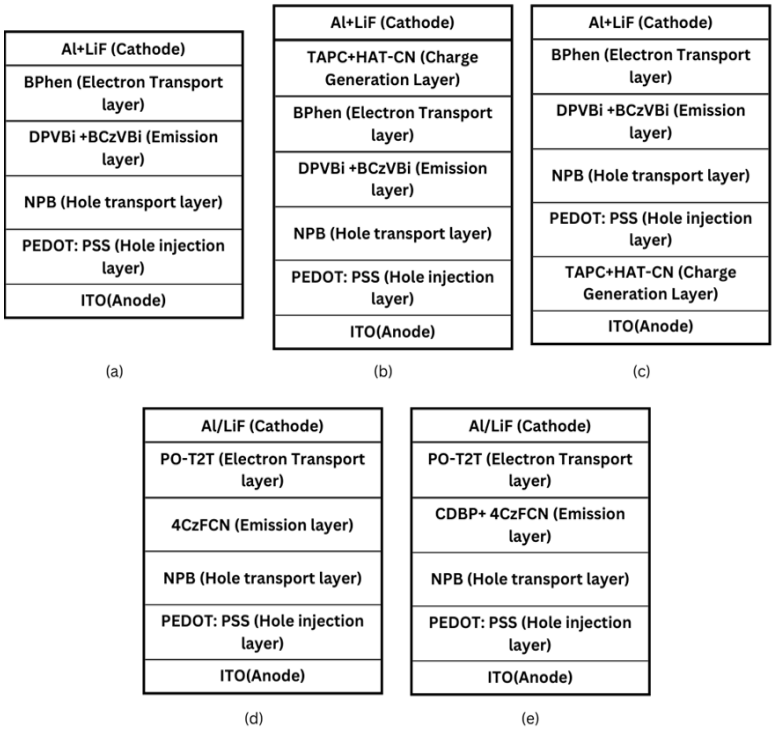

Figure 1. a) Reference device A with no charge generation layers, b) Device B with CGL below cathode, c) Device C with CGL above anode, d)Device D with neat TADF emitter and e) Device E with CDBP doped emitter.

This particular device is designated as Device A, as illustrated in Fig. 1a. Notably, this reference device, Device A, does not comprise a charge generation layer. Following these layers, charge generation layers (CGL) are integrated into the device architecture. Initially, the charge generation layer TAPC (Hole generator) and HAT-CN (Electron generator) are incorporated into the device, positioned beneath the cathode. This configuration is identified as Device B, as depicted in Fig. 1b. Subsequently, a charge generation layer is situated above the anode, designating it as Device C. It is evident that the luminescence of Device B surpasses that of Device A, attributable to the presence of the CGL, which is capable of generating a greater quantity of free charge carriers. These charge carriers ultimately facilitate recombination within the emissive layer. Among all the devices evaluated, Device C yields the most favorable results, as the free electrons within HAT-CN are attracted from the anode side, while concurrently, the free holes in TAPC are drawn away from the anode towards the emissive layer (EML).

Moreover, in the domain of organic electronics, the mobility of holes is superior when juxtaposed with that of electrons. Consequently, in this scenario, the concentration of holes will exhibit a more pronounced increase relative to Device B, wherein the charge generation layer (CGL) is situated in proximity to the cathode. Thus, the recombination rate in Device C is anticipated to surpass that of Device B for the aforementioned reasons [28], [29]. In the fabrication of thermally activated delayed fluorescence (TADF) organic light-emitting diodes (OLEDs), ITO-coated glass substrates undergo a solution cleaning process followed by a 15-minute ultraviolet exposure to modify the surface characteristics and work function, thereby serving as the anode. Following an annealing step at 120◦C to drive off any solvent traces, a fine layer of poly(3,4-ethylenedioxythiophene):polystyrene sulfonate (PEDOT:PSS) is formed and deposited onto a tailored ITO-coated glass surface using solution-processing, acting as the hole-injection layer (HIL). N,N’-Bis(naphthalen-1-yl)-N,N’-bis(phenyl)-benzidine (NPB) is treated with heat at 100◦C to remove leftover solvents, forming a thin hole-transporting

layer (HTL); 2,3,4,6-tetrakis(9H-carbazole-9-yl)- 5-fluorobenzonitrile (4CzFCN) acts as a deep blue TADF emitter to create a clean emissive layer, while 2,4,6-Tris[3-(diphenylphosphinyl)phenyl]-1,3,5-triazine (PO-T2T) functions as the electron transporting layer, with lithium fluoride and aluminum serving as the cathode, which is crafted through a dry method (physical vapor deposition). This configuration represents Device D, as illustrated in Fig. 1d. Subsequently, 4,4'-Bis(9-carbazolyl)-2,2'-dimethylbiphenyl (CDBP) is doped with 4CzFCN to create a doped emissive layer, resulting in Device E depicted in Fig. 1e. It is evident that the luminescent performance of Device E surpasses that of Device D, as it incorporates a doped emissive layer (EML) that is attributed to enhanced carrier concentrations. This ultimately leads to a 28% increase in the recombination rate in Device E compared to Device D. Among these five devices, Device E yields the most favorable outcomes, as it represents a third-generation doped thermally activated delayed fluorescence OLED.

Characteristic parameters

An effective method for analyzing electronic equipment is analytical modeling. It makes it possible to fully understand the intricate physics underlying the device [30]. Numerous characteristic factors define an OLED's performance and help determine its viability for a particular application. A number of characteristics are important when assessing an OLED's suitability for a range of applications, including electric field, luminescence, current density, external quantum efficiency, power efficiency, and current efficiency. These properties are influenced by a wide range of factors, including the device's architecture, the electrodes, various supporting layers, the emission material (phosphorescence or fluorescence), the electron and hole mobilities, and more. For an OLED, these parameters must typically reach relatively high values [31].

a) The equations utilized to stimulate the fluorescent OLEDs are as follows:

Poisson's equation is employed to investigate the internal characteristics and to compute the electric field of the OLED, which emerges due to the distribution of charge density within the organic device when the applied electric field is known. The equation is articulated as delineated in the following expression:

$$E(z+\Delta z/2,t) = E(z-\Delta z/2,t) + N_D(z) - N_A(z) + \Delta z \cdot (q/\varepsilon) \cdot \big(p(z,t) - n(z,t)\big) \quad (1)$$

In this formulation, Δz represents the width in centimeters of each mesh or cell. The entire device is separated into several of these cells, which are mesh points where various computations are performed. E(z, t) represents the electric field at each of these mesh points; q and ε represent the electron charge and permittivity, respectively; p(z, t) and n(z, t) represent the electron and hole concentrations as functions of z and t; and t is the time interval for which the calculations are carried out. Lastly, NA(z) and ND(z) display the concentrations of donor and acceptor impurities at position z within the device. Consequently, at every mesh point on the apparatus, the electric field is updated.

The Poole-Frenkel mobility model explains the hopping-type carrier transport observed in organic semiconductors (OSCs). The mobility variation brought on by the effective electric field is computed for each mesh point on the apparatus. The Poole-Frenkel mobility model can be derived from the following statement:

$$\mu(E) = \mu_0 \exp\left[-\frac{\Delta}{kT} + \left(\frac{\beta}{kT} - \alpha\right)\sqrt{E}\right] \quad (2)$$

Here, the zero-field mobility, denoted by μ0, and the field-dependent mobility, denoted by μ(E), fluctuate in response to variations in the applied electric field. Temperature (K) and the Boltzmann constant (J/K) are represented by the variables K and T, respectively. Furthermore, the activation energy at zero field is represented by Δ, and α is utilized as a fitting parameter. Lastly, the letter E stands for the applied electric field. The hole Poole–Frenkel factor β is defined as follows:

$$\beta = q\sqrt{\frac{q}{\pi\varepsilon\varepsilon_0}} \quad (3)$$

Langevin's recombination model delineates the electron and hole recombination process within the OLED. Due to their relatively low mobilities, organic devices do not adhere to conventional recombination processes. The Langevin's recombination model is articulated in the following equation:

$$R_L(n,p) = r_l(x,y,t)(np - n_i^2) \quad (4)$$

Here, r1 represents Langevin's recombination rate coefficient, while ni symbolizes the intrinsic carrier concentration. The variables p and n denote the concentrations of holes and electrons, respectively. The Langevin's recombination rate is further calculated from the following expression:

$$r_l(x,y,t) = \frac{q\mu(E)}{\varepsilon_r\varepsilon_0} \quad (5)$$

where q denotes the fundamental charge associated with an electron. The parameter of relativity and absolute permittivity are represented by ε_r and ε_0 respectively.

b) The TADF OLEDs are activated through the application of the subsequent equations.

The drift-diffusion equations elucidate the current-density J pertaining to holes and electrons, which can be articulated in the following manner.

$$J_p = q\mu_p p \frac{d}{dx}\left(\frac{E_{\text{HOMO}}}{q}\right) - qD_p \frac{dp}{dx} \quad (6)$$

$$J_n = q\mu_n n \frac{d}{dx}\left(\frac{E_{\text{LUMO}}}{q}\right) - qD_n \frac{dn}{dx} \quad (7)$$

In this case, μp and μn represent the hole and electron mobilities, respectively, and Jp and Jn represent the current-density of holes and electrons. Additionally, Dp and Dn stand for the diffusion coefficients for holes and electrons, respectively. Tunneling events and thermionic emission are the two primary components of the electron current density. The overall current density can be estimated using the formula below:

$$J_{nb} = qv_{rn}(n_b - n_{qe}) + J_{ntu} \quad (8)$$

The electron density at the contact interface is denoted by nb, the quasi-equilibrium current density at the contact by nqe, and the surface recombination velocity by vrn.

The output brightness of organic light-emitting diodes is a crucial indicator of their operational efficacy. Luminosity is the amount of light emitted per unit area, measured in candelas per square meter (cd/m2). The following equation can also be used to determine the photometric evaluation of light that is impinging on a unit area and propagating in a specific direction.

$$L = K_m \int_\lambda \eta_{cp} I_{EL_{tot}}(\lambda) V(\lambda)\ d \quad (9)$$

In this equation, Km =683 lm/W is the constant power efficacy pertinent to the photopic human visual system, η_{cp} represents the outcoupling efficiency, and V (λ) indicates the relative spectral sensitivity of the human eye.

The continuity equation elucidates the temporal dynamics characterizing the concentrations of holes and electrons, accounting for the processes of generation, recombination, and the resultant current flow. The recombination rate can be articulated through the following continuity equations.

$$\frac{\partial n}{\partial t} = \frac{1}{q}\frac{dJ_n}{dx} + G_n - R \quad (10)$$

$$\frac{\partial p}{\partial t} = \frac{1}{q}\frac{dJ_p}{dx} + G_p - R \quad (11)$$

In this formulation, Gn and Gp stand for the electron and hole creation rates, respectively, and R for the recombination rate. Efficiency roll-off is reduced in devices with a larger recombination zone, among other benefits. The efficiency roll-off phenomenon is a major issue with organic light-emitting diodes (OLEDs) that use thermally activated delayed fluorescence (TADF). Even though lowering the singlet-triplet energy gap (ΔEST) has historically been employed as a tactic, a new figure of merit for material design is proposed to reduce roll-off while taking into account the dynamic equilibrium between singlet and triplet states. Despite their potential as a phosphorescent emitter substitute, TADF materials frequently experience significant efficiency losses at high drive currents. Contrary to earlier research that assumed that the singlet-triplet energy gap (ΔEST) and the reverse intersystem crossing rate (kRISC) would effectively reduce roll-off, the authors discovered that these parameters are insufficient to fully explain the phenomenon, which is fundamental to the physics of hyperfluorescent OLEDs (Fourth Generation OLED). By examining the dynamic equilibrium between singlets and triplets in TADF materials, the authors present a novel figure of merit for materials design. This measure is intended to support the development of TADF materials with lower efficiency roll-off in order to enhance OLED performance under realistic operating conditions and increase their use in high-brightness applications such as lighting, augmented reality, and lasing [11], [32].

Triplet-triplet annihilation (TTA) is the main cause of roll-off in single-layer TADF OLEDs, according to Zee et al. (2021) [33]. According to Zhang et al. (2019), roll-off from singlet-triplet annihilation and TTA can be successfully reduced by building an emitting layer with dual delayed fluorescence [34]. TADF decay rates and photoluminescence quantum efficiencies with efficiency roll-off are correlated by Hasan et al. (2022), suggesting that lowering delayed or prompt lifetimes and increasing their respective contributions can lead to higher external quantum efficiency and lower roll-off in TADF OLEDs [35].

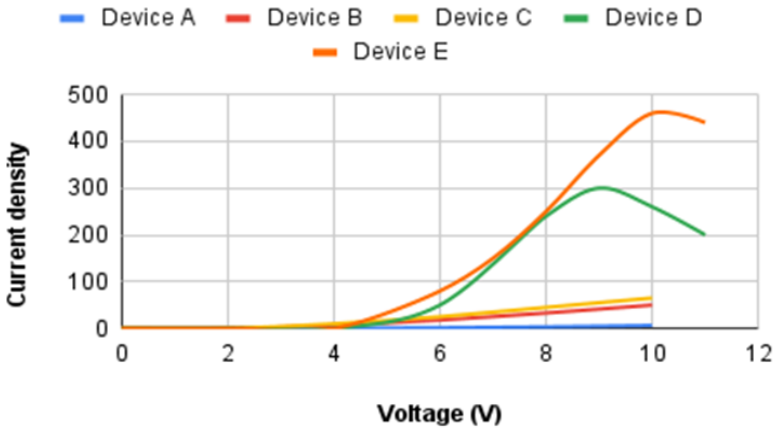

Figure 2. Comparison of Current density vs Voltage (Applied Voltage) characteristics in whole devices

For 1st generation OLEDs, three devices, i.e. Device A, Device B, and Device C-are considered. Figure 2 shows the comparison of Current density vs Voltage (Applied Voltage) characteristics in whole devices. Figure 3 display comparison of Luminance vs Voltage (Applied Voltage) characteristics in whole devices. Figure 4 demonstrates the comparison of Recombination rate vs Distance characteristics in whole devices.

In order to achieve a recombination rate and luminescence of 215.9 cd/m^2, 1×10^6 /cm^{3}s, Device A maintains a current density of 6.5 mA/cm^2. With features like a current density of 50 mA/cm^2, luminescence of 1592.3 cd/m^2, and a recombination rate of 2×10^6 /cm^{3}s, Device B also behaves better. With a current density of 65 mA/cm^2, enhanced luminescence of 2112.2 cd/m^2, and a recombination rate of 5.5 × 10^6 /cm^{3}s, Device C is the best of the first-generation samples [28].

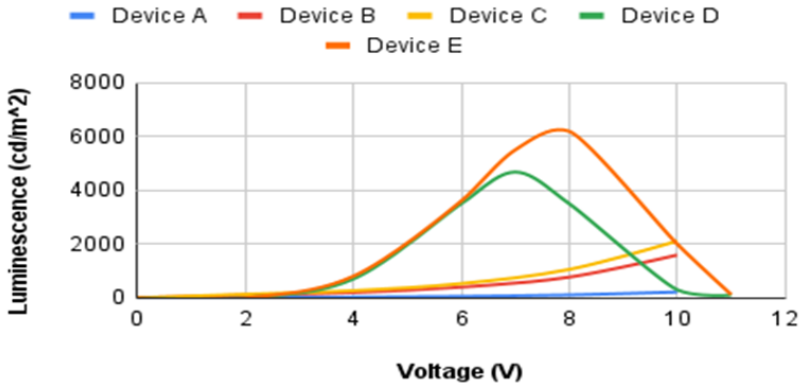

Figure 3. Comparison of Luminance vs Voltage (Applied Voltage) characteristics in whole devices

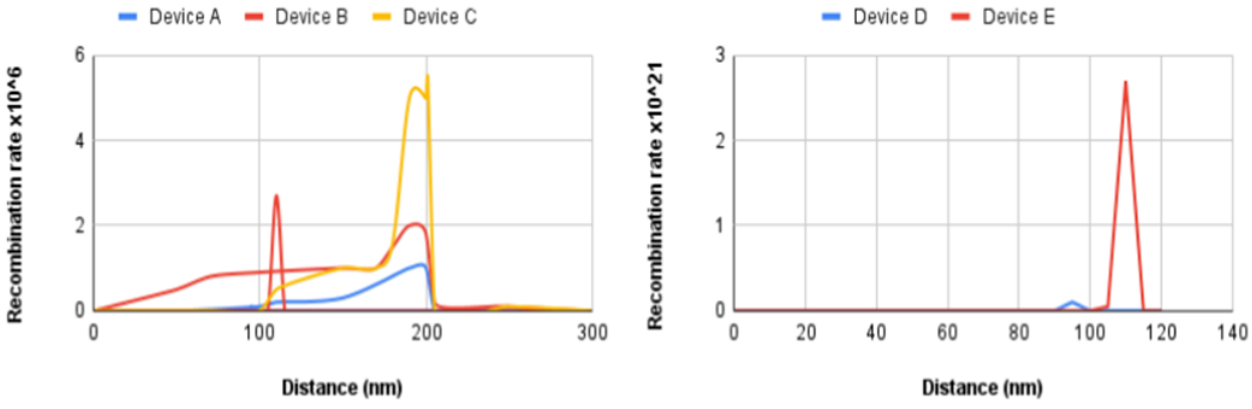

Figure 4. Comparison of Recombination rate vs Distance characteristics in whole devices

Compared to them, 3rd Generation OLEDs like Device D and Device E, have much better performance. Device D has an extremely high current density of 310 mA/cm^2, yet a luminescence of only 4678 cd/m^2, with recombination rate doubling to 10^{21} /cm^{3}s. Device E takes these higher still with 460 mA/cm^2 current density, an exceedingly high luminescence of 6192 cd/m^2, and a recombination rate of 2.7×10^{21} /cm^{3}s. This stark contrast between the 1st and 3rd generation OLEDs highlights the significant advancements in device engineering, specifically in charge carrier dynamics and radiative recombination efficiency. The enhancement in the rates of recombination from the order of 10^6 to 10^{21} /cm^{3}s reflects the upgraded material and structural characteristics in 3rd Gen OLEDs, attributed to the use of Thermally Activated Delayed Fluorescence (TADF) emitters [36].

2. CONCLUSION

In summary, the comparative examination of third-generation thermally activated delayed fluorescence (TADF) organic light-emitting diodes (OLEDs) exhibit significant advancements over first- and second-generation devices, particularly in biomedical diagnostics and phototherapy for ovarian cancer. This study evaluates five devices (A–E): Device A is non-CGL-based, devices B and C are CGL-based, and devices D and E are TADF-based, with D functioning as a neat emitter and E as a doped emitter. Incorporating TADF materials like carbazole derivatives, which utilize both singlet and triplet excitons, offers a theoretical external quantum efficiency of up to 100%. Amongst all devices, Device E demonstrates the highest performance, achieving a current density of 460 mA/cm², luminescence of 6192 cd/m², and a recombination rate of 2.7×10^{21}. TADF OLEDs' distinctive optical properties enhance cancer biomarker detection sensitivity, supporting improved diagnostic and therapeutic strategies. However, challenges such as efficiency roll-off at high drive currents persist, underscoring the need for further exploration into material stability and device architecture optimization. Interdisciplinary efforts are crucial to advancing TADF OLED technology, enabling innovative applications in personalized medicine and better treatment outcomes. Future work includes developing novel emitter materials, optimizing device structures, integrating nanostructured substrates, and exploring hybrid systems. These advancements aim to improve efficiency and stability while promoting sustainable, cost-effective manufacturing processes, broadening TADF OLED technology's application across various sectors.

REFERENCES

[1] Geffroy B, Le Roy P, Prat C. Organic light-emitting diode (OLED) technology: materials, devices and display technologies. Polymer international. 2006 Jun;55(6):572-82.

[2] Sasabe H, Kido J. Development of high-performance OLEDs for general lighting. Journal of Materials Chemistry C. 2013;1(9):1699-707.

[3] Shirota Y, Kageyama H. Charge carrier transporting molecular materials and their applications in devices. Chemical reviews. 2007 Apr 11;107(4):953-1010.

[4] Moral M, Muccioli L, Son WJ, Olivier Y, Sancho-Garcia JC. Theoretical rationalization of the singlet–triplet gap in OLEDs materials: impact of charge-transfer character. Journal of Chemical Theory and Computation. 2015 Jan 13;11(1):168-77.

[5] Du C, Liu H, Cheng Z, Zhang S, Qu Z, Yang D, Qiao X, Zhao Z, Lu P. Ultraefficient non-doped deep blue fluorescent OLED: achieving a high EQE of 10.17% at 1000 cd m-2 with CIEy< 0.08. Advanced Functional Materials. 2023 Nov;33(45):2304854.

[6] Klimes K, Zhu ZQ, Li J. Efficient blue phosphorescent OLEDs with improved stability and color purity through judicious triplet exciton management. Advanced Functional Materials. 2019 Aug;29(31):1903068.

[7] Rajamalli P, Senthilkumar N, Gandeepan P, Ren-Wu CC, Lin HW, Cheng CH. A method for reducing the singlet–triplet energy gaps of TADF materials for improving the blue OLED efficiency. ACS applied materials & interfaces. 2016 Oct 12;8(40):27026-34.

[8] Prabowo BA, Su LC, Chang YF, Lai HC, Chiu NF, Liu KC. Performance of white organic light-emitting diode for portable optical biosensor. Sensors and Actuators B: Chemical. 2016 Jan 1;222:1058-65.

[9] Jeon Y, Choi HR, Park KC, Choi KC. Flexible organic light-emitting-diode-based photonic skin for attachable phototherapeutics. Journal of the Society for Information Display. 2020 Apr;28(4):324-32.

[10] Romano G, Insero G, Marrugat SN, Fusi F. Innovative light sources for phototherapy. Biomolecular Concepts. 2022 May 23;13(1):256-71.

[11] Diesing, S.; Zhang, L.; Zysman-Colman, E.; Samuel, I.D.W. A figure of merit for efficiency roll-off in TADF-based organic LEDs. Nature 2024, 627, 747–753.

[12] Sem, S.; Jenatsch, S.; Sahay, P.; Züfle, S.; Schmid, M.; Brütting, W.; Ruhstaller, B. Detailed electro-optical modeling of thermally-activated delayed fluorescent OLEDs with different host-guest concentrations. Organic Electronics 2022, 107, 106553.

[13] Negi, S.; Mittal, P.; Kumar, B. Modeling and analysis of high-performance triple hole block layer organic LED based light sensor for detection of ovarian cancer. IEEE Transactions on Circuits and Systems I: Regular Papers 2021, 68, 3254–3264.

[14] Negi, S.; Mitta, P.; Kumar, B.; Bhatia, A. Detection of Ovarian Cancer using Organic Light Emitting Diodes. In Proceedings of the 2018 5th IEEE Uttar Pradesh Section International Conference on Electrical, Electronics and Computer Engineering (UPCON). IEEE, 2018, pp. 1–4.

[15] Gunaydin, G.; Gedik, M.E.; Ayan, S. Photodynamic therapy for the treatment and diagnosis of cancer–a review of the current clinical status. Frontiers in chemistry 2021, 9, 686303.

[16] Hong, G.; Gan, X.; Leonhardt, C.; Zhang, Z.; Seibert, J.; Busch, J.M.; Bräse, S. A brief history of OLEDs—emitter development and industry milestones. Advanced Materials 2021, 33, 2005630.

[17] Huang, Y. Recent research of materials for emissive layer of OLED. In Proceedings of the Journal of Physics: Conference Series. IOP Publishing, 2023, Vol. 2608, p. 012012.

[18] Liu, Z. A Compact History of the OLEDs. Applied and Computational Engineering 2023, 3, 350–355.

[19] Silviu, P. ORGANIC LIGHT EMITTING DIODES (OLED). Annals of the Academy of Romanian Scientists Series on Physics and Chemistry 2023, 8, 46–57.

[20] Zhang, C.; Zhang, D.; Bin, Z.; Liu, Z.; Zhang, Y.; Lee, H.; Kwon, J.H.; Duan, L. Color-tunable all-fluorescent white organic light-emitting diodes with a high external quantum efficiency over 30% and extended device lifetime. Advanced Materials 2022, 34, 2103102.

[21] Huang, Z.; Xie, H.; Miao, J.; Wei, Y.; Zou, Y.; Hua, T.; Cao, X.; Yang, C. Charge transfer excited state promoted multiple resonance delayed fluorescence emitter for high-performance narrowband electroluminescence. Journal of the American Chemical Society 2023, 145, 12550–12560.

[22] Ye, J.; He, Y.; Li, K.; Liu, L.; Xi, C.; Liu, Z.; Ma, Y.; Zhang, B.; Bao, Y.; Wang, W.; et al. Achieving record efficiency and luminance for TADF light-emitting electrochemical cells by dopant engineering. ACS Applied Materials & Interfaces 2022, 14, 17698–17708.

[23] Wang, Y.Y.; Tong, K.N.; Zhang, K.; Lu, C.H.; Chen, X.; Liang, J.X.; Wang, C.K.; Wu, C.C.; Fung, M.K.; Fan, J. Positive impact of chromophore flexibility on the efficiency of red thermally activated delayed fluorescence materials. Materials Horizons 2021, 8, 1297–1303.

[24] Tai, J.W.; Tang, Y.; Zhang, K.; Yang, C.Z.; Pan, Z.H.; Lin, Y.C.; Shih, Y.W.; Chen, C.H.; Chiu, T.L.; Lee, J.H.; et al. 13.2% EQE near-infrared TADF OLED with emission peak at 761 nm. Chemical Engineering Journal 2023, 452, 139534.

[25] Balijapalli, U.; Nagata, R.; Yamada, N.; Nakanotani, H.; Tanaka, M.; D'Aléo, A.; Placide, V.; Mamada, M.; Tsuchiya, Y.; Adachi, C. Highly efficient near-infrared electrofluorescence from a thermally activated delayed fluorescence molecule. Angewandte Chemie International Edition 2021, 60, 8477–8482.

[26] Liu, Y.; Yang, J.; Mao, Z.; Chen, X.; Yang, Z.; Ge, X.; Peng, X.; Zhao, J.; Su, S.J.; Chi, Z. Asymmetric thermally activated delayed fluorescence emitter for highly efficient red/near-infrared organic light-emitting diodes. ACS Applied Materials & Interfaces 2022, 14, 33606–33613.

[27] Wang, S.; Yan, X.; Cheng, Z.; Zhang, H.; Liu, Y.; Wang, Y. Highly efficient near-infrared delayed fluorescence organic light emitting diodes using a phenanthrene-based charge-transfer compound. Angewandte Chemie International Edition 2015, 54, 13068–13072.

[28] Negi, S.; Mittal, P.; Kumar, B. Impact of different layers on performance of OLED. Microsystem Technologies 2018, 24, 4981–4989.

[29] Yadav, S.; Mittal, P.; Negi, S. Positional Analysis and Comparison of Different Charge Generation Layer Based Blue OLEDs. In Proceedings of the 2024 2nd International Conference on Device Intelligence, Computing and Communication Technologies (DICCT). IEEE, 2024, pp. 644–649. 378

[30] Negi, S.; Mittal, P.; Kumar, B. Analytical modelling and parameters extraction of multilayered OLED. IET Circuits, Devices & Systems 2019, 13, 1255–1261.

[31] Negi, S.; Mittal, P.; Kumar, B. In-depth analysis of structures, materials, models, parameters, and applications of organic light-emitting diodes. Journal of Electronic Materials 2020, 49, 4610–4636.

[32] Rodella, F.; Saxena, R.; Bagnich, S.; Banevicˇius, D.; Kreiza, G.; Athanasopoulos, S.; Jursenas, S.; Kazlauskas, K.; Köhler, A.; Strohriegl, P. Low efficiency roll-off blue TADF OLEDs employing a novel acridine–pyrimidine based high triplet energy host. Journal of Materials Chemistry C 2021.

[33] van der Zee, B.; Li, Y.; Wetzelaer, G.J.A.; Blom, P.W. Origin of the Efficiency Roll-Off in Single- 387 Layer Organic Light-Emitting Diodes Based on Thermally Activated Delayed Fluorescence. 388 Advanced Optical

Materials 2021, 9, 2100249.

[34] Zhang, Y.; Li, Z.; Li, C.; Wang, Y. Suppressing efficiency roll-off of TADF based OLEDs by constructing emitting layer with dual delayed fluorescence. Frontiers in Chemistry 2019, 7, 302.

[35] Hasan, M.; Shukla, A.; Mamada, M.; Adachi, C.; Lo, S.C.; Namdas, E.B. Correlating exciton dynamics of thermally activated delayed-fluorescence emitters to efficiency roll-off in OLEDs. Physical Review Applied 2022, 18, 054082.

[36] Tiwari, R.K.; Mishra, R.; Sharma, S.K.; Prabhu, N.; Nagar, M.R.; Grigalevicius, S. Advancing Cancer Treatment and Diagnosis: A Review on Photodynamic Therapy Using OLED Technology. Molecules 2025, 30, 1305